Estimating the Unloaded Quality Factor of Reverberation Chambers Using the Effective Conductivity Model

Qian Xu, *Member, IEEE*, Lei Xing, *Member, IEEE*, Yongjiu Zhao, Xinlei Chen, *Member, IEEE*, Yi Huang, *Fellow, IEEE*, Xueqi Shen, Mark Paul Leach, *Member, IEEE*, Eng Gee Lim, *Senior Member, IEEE*, and Tian-Hong Loh, *Senior Member, IEEE*

***Abstract*—Estimating the *Q* factor of an unloaded reverberation chamber (RC) is a challenging problem in practice. To answer this question conservatively and confidently, this paper reviews the measured unloaded *Q* factors of 38 RCs worldwide. The effective wall conductivities are summarized from the reported measurement results. Broadband *Q* factors of RCs from the same supplier but with different dimensions are highlighted to compare. The measurement results show that the effective wall conductivity is frequency dependent and the dependency behaves in a similar way. The empirical values of the effective wall conductivity are extracted to estimate the unloaded *Q* factors conservatively.**

***Index Terms*—Reverberation chamber, *Q* factor.**

I. Introduction

REVERBERATION chambers (RCs) are over-mode cavities with stirrers which can tune the electromagnetic fields inside the cavities randomly by moving the stirrers either in continuous or discrete manner. RCs have been widely used in electromagnetic compatibility (EMC) for decades [1]-[3] and have been expanded into over-the-air (OTA) testing of wireless devices in recent years [4]. In RC EMC applications, a frequently asked question from the costumers in industry is: what is the mean/highest electric field (E-field) an RC can achieve for 1 W input power? For a commercially off-the-shelf RC, as it would have been measured, a typical E-field curve can be given. However, for an RC with customized dimensions, it may not be easy to answer the question quickly. It is well known that the key is the quality (*Q*) factor.

The *Q* factor of an RC is an important figure of merit to describe its ability to store energy. It is defined as [5]

$$Q = \omega \frac{\bar{W}}{P_d} \tag{1}$$

where $\bar{W}$ is the time-averaged total stored energy in the RC, $\omega = 2\pi f$ is the angular frequency, and P_d is the dissipated power. The *Q* factor characterizes the resonance of the cavity and determines the mean E-field strength for a given input power.

Obviously, when all the losses in an RC are quantified, the *Q* factor can be simulated accurately. However, estimating accurate *Q* factors without measurements could be extremely difficult, as the losses in practice could be far off from the parameters in simulations. Because there are connections between panels, screws, dirt and possible oxidation spots, the effective conductivity of the walls could be much less than the conductivity of pure material [6]. Although the *Q* factor may not be a big issue in OTA measurements (the chamber transfer function is calibrated in measurements and not very high E-field is required [4]), in EMC radiated susceptibility testing, the *Q* factor determines the highest acquired E-field the RC can achieve. The *Q* factor can only be reduced (e.g. using absorbing materials) once an RC is built, as the unloaded *Q* factor is envisaged as the maximum *Q* factor value of the RC.

Several computational electromagnetics (CEM) tools have been employed for RC simulations to provide important insights over the last decades. For example, the finite-difference time-domain (FDTD) has been used to simulate the stirrer performance [7]-[10], field uniformity [9], [10], independent sample number [9], [10] and the loss effect [11]-[15]. It has been found that the volumetric loss can be used to emulate the total loss in an RC [11]-[15], and a typical value of air conductivity of 10^{-5} S/m can be used for galvanized steel RCs [12]-[15]. However, this empirical value is limited in a certain frequency range. Similarly, the transmission line matrix (TLM) method has been applied in [16]-[20] for the analysis and optimization of the RC designs. Frequency domain methods such as boundary element method (BEM) [21], [22],

Manuscript received **.

Q. Xu, L. Xing, Y. Zhao and X. Chen are with College of Electronic and Information Engineering, Nanjing University of Aeronautics and Astronautics, Nanjing 211106, China (e-mail: emxu@foxmail.com).

Y. Huang is with the Department of Electrical Engineering and Electronics, The University of Liverpool, Liverpool, L69 3GJ, UK. (e-mail: yi.huang@liverpool.ac.uk).

M. P. Leach and E. G. Lim are with the Department of Electrical and Electronics Engineering, Xi'an Jiaotong Liverpool University, Suzhou, 215123, China (e-mail: Mark.Leach@xjtlu.edu.cn; enggee.lim@xjtlu.edu.)

X. Shen is with Nanjing Rongce Testing Technology Ltd, Nanjing, 211112, China (e-mail: george@emcdir.com).

T. –H. Loh is with Electromagnetic & Electrochemical Technologies Department, 5G & Future Communications Technology Group, National Physical Laboratory, Teddington, TW11 0LW, UK. (e-mail: tian.loh@npl.co.uk).

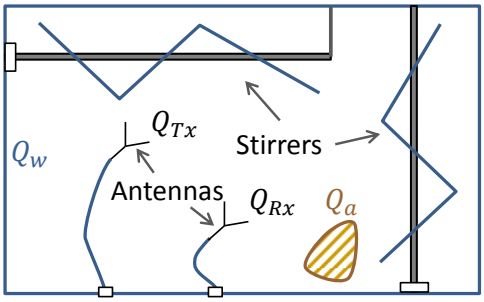

Fig. 1. Typical measurement setup in an RC.

method of moments (MoM) [23]-[29], fast multipole method (FMM) and multilevel fast multipole method (MLFMM) [30]-[32] can take the advantage of surface discretization and could be more efficient for irregularly shaped and rotating structures. The finite element method (FEM) may not be very efficient in analyzing the broadband frequency response of RCs at high frequencies, but it can be used for low frequency simulation and eigenanalysis [33]-[43].

It has been found that as long as the simulated RC *Q* factor is realistically close to its practical value, the behavior of an RC can be modeled accurately from a statistical perspective (without considering the time and resource consumption) [44]. Note that one needs to measure the *Q* factor first and fit the parameters later in simulations. For a commercial off-the-shelf RC, the unloaded *Q* factor could have already been evaluated thereby; the loaded E-field can be estimated from the absorption cross section (ACS) of the loaded object [45], [46]. However, establishing a customized RC without such evaluation, the accurate estimation of loaded E-field could be extremely difficult to simulate all the loss just from pure simulation. In this paper, we aim to solve this problem by applying an engineering approach: analyzing measurement results from the existing RCs directly, a conservative estimation of the effective wall conductivity can be obtained for RCs with galvanized steel walls, thus the problem can be empirically answered.

This paper is organized as follows. Section II provides the theory; Section III summarizes the *Q* factors of the RCs from the published literatures, while we have also measured *Q* factors of three RCs with different dimensions from the same supplier; typical effective conductivity is summarized for RCs with galvanized steel walls. Section IV provides the discussion and the equivalency with the lossy air model. Section V concludes the paper.

II. Theory

The loss mechanism in an RC has been detailed in [5]. A typical setup for the *Q* factor measurement is illustrated in Fig. 1, the overall average *Q* factor can be decomposed as

$$Q^{-1} = Q_w^{-1} + Q_{Tx}^{-1} + Q_{Rx}^{-1} + Q_a^{-1} \tag{2}$$

where Q_w is the contribution from the finite conductivity of the walls, ceilings and ground, Q_{Tx} , Q_{Rx} and Q_a are the contributions from transmitting (Tx) antenna, receiving (Rx) antenna and lossy objects loaded in the RC, respectively. As the shielding effectiveness of an RC is normally very good, the contribution from the aperture transmission cross section in (2) is not being considered. The expressions for the decomposed *Q* factors are

$$Q_w = \frac{3V}{2\mu_r S\delta_w}\frac{1}{1+\frac{3\pi}{8k}\left(\frac{1}{a}+\frac{1}{b}+\frac{1}{d}\right)} \tag{3}$$

$$Q_{Tx} = \frac{8\pi^2 V}{m\lambda^3} \tag{4}$$

$$Q_{Rx} = \frac{16\pi^2 V}{m\lambda^3} \tag{5}$$

$$Q_a = \frac{2\pi V}{\lambda\langle \mathrm{ACS}\rangle} \tag{6}$$

$$\delta_w = \sqrt{2/(\omega\mu\sigma_{\mathrm{eff}})} \tag{7}$$

where V is the volume of the RC, $\mu_r \approx 1$ is the relative permeability of the RC walls, S is the overall inner surface area of the RC, δ_w is the skin depth, $k = 2\pi/\lambda$ is the wavenumber,

TABLE I
RCs with Different Dimensions

Index	Dimensions (m)	Volume (m^3)	References
#1	0.3×0.25×0.15	0.013	[52]
#2	0.42×0.41×0.38	0.067	[53]
#3	Surface area: 1.25 m^2	0.08	[54]
#4	0.58×0.59×0.60	0.204	[55]
#5	0.8×0.8×1.2	0.769	[56]
#6	1.49×1.16×1.45	2.51	[57]
#7	2.48×1.87×2.48	11.5	[58]
#8	3.8×2.3×1.5	13.1	[6]
#9	3.08×1.84×2.44	13.8	[59]
#10	2.9×2.13×2.72	16.8	[60]
#11	2.48×2.48×2.86	17.6	[61]
#12	2.95×2.75×2.35	19.1	[61]
#13	2.5×2.5×3.1	19.4	[62]
#14	3.7×2.5×2.89	26.7	[63]
#15	4.9×2.5×3	36.8	[21]
#16	2.74×3.05×4.57	38.2	[60]
#17	2.9×4.2×3.6	13.8	[64]
#18	5.8×3.2×2.4	44.5	[65]
#19	3×5.4×2.8	45.4	-
#20	5.3×3.7×3	58.8	[28]
#21	6×4×2.5	60.0	[66]
#22	3.9×6×2.8	65.5	-
#23	4.05×5.7×3.15	72.7	[67]
#24	6.16×4.05×3.15	78.6	[68]
#25	2.9×3.96×7.01	80.5	[60]
#26	5.8×4×3.6	83.5	[69], [70]
#27	2.9×3.7×8.7	93.4	[71]
#28	7.78×4.34×3.1	105	[57]
#29	6.55×5.85×3.5	134	[72], [73]
#30	7.9×6.5×3.5	180	[74]
#31	7.5×5.6×4.6	193	[6]
#32	8.94×6×3.92	210	[75]
#33	2.9×7.01×14.33	291	[60]
#34	10.5×8×4.3	361	[76]
#35	12.6×10.8×6.03	821	[46]
#36	29×11×6	1914	[77], [78]
#37	8×14.7×20	2352	[79]
#38	Surface area: 5735 m^2	23315	[80]

#3 and #38 are not rectangular RCs, #19 and #22 are chambers introduced in this paper.

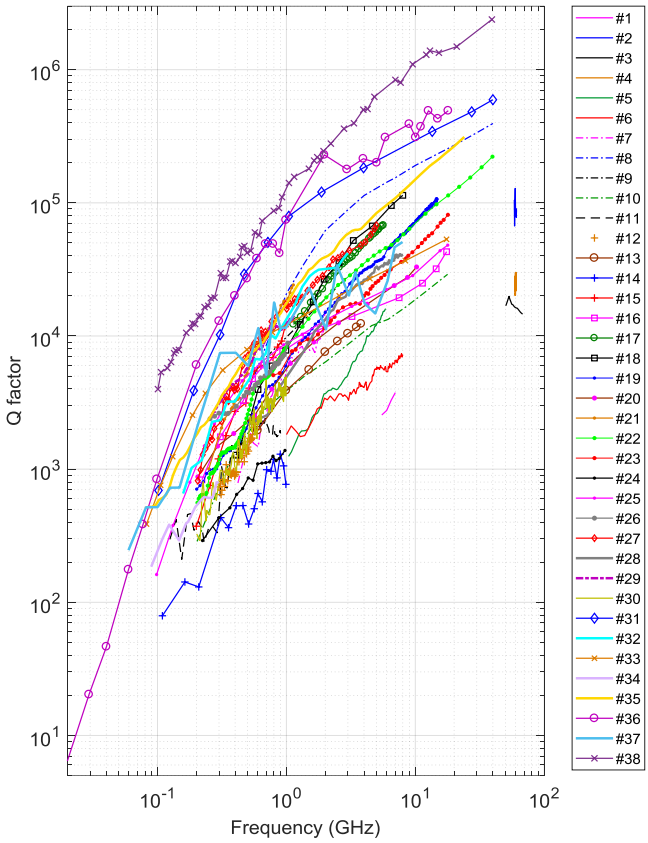

Fig. 2. Measured Q factors extracted from references.

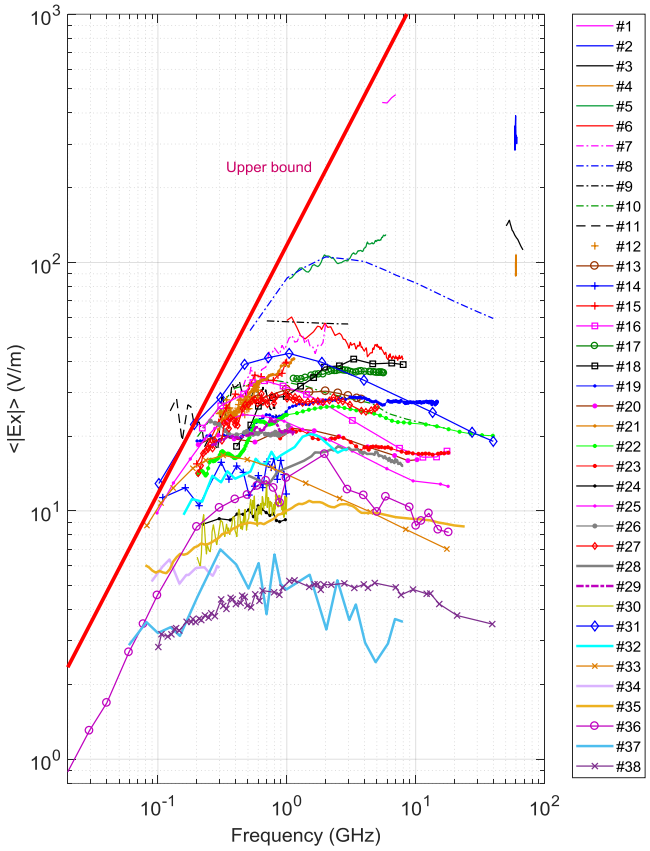

Fig. 3. The normalized E-field (net input power is 1 W) calculated from the Q factor and the volume of the RCs, the upper bound is also given.

λ is the wavelength, m is the impedance mismatch factor, $\langle ACS \rangle$ is the average ACS of the loading object, ω is the angular frequency, $\mu = \mu_r \mu_0$ is the permeability of the RC walls, $\mu_0 = 4\pi \times 10^{-7}$ H/m is the permeability of free space, σ_{eff} is the effective conductivity of the RC walls, a, b and d are the width, length and height of a rectangular RC, respectively.

Because of the enhanced back scatter effect, when an RC is well stirred, the average power absorbed by the Tx antenna is twice of that absorbed by the Rx antenna [6], [47]-[49]. We assume Q_a does not dominate the Q factor of the RCs (unloaded) and the antennas are well matched in the published literatures, by applying $m \approx 1$ and $Q_a^{-1} \approx 0$ in (2)-(7), the effective conductivity of the walls can be solved from the measured overall average Q factor.

Note that at high frequencies, the loss of the antennas does not dominate the Q factor, even the contribution of Q_{Tx}, Q_{Rx} and Q_a are not considered, the results remain similar [6], [50]. The detailed structure does not affect the loss of the walls at high frequency, and Q_w in (3) can be further simplified to $Q_w = 3V/(2\mu_r S \delta_w)$ [5], [51].

III. Measurement Data

After reviewing the published literatures, the RCs with different dimensions are listed in Table I. They are sorted with ascending volumes which works from millimeter wave frequencies to frequencies lower than 80 MHz. The measured Q factors are extracted and illustrated in Fig. 2. The mean E-field strength can be calculated using [3], [5]

$$\langle |E_x| \rangle_u = \sqrt{\frac{5\pi Q \lambda P_{in}}{V}} \tag{8}$$

where $\langle |E_x| \rangle_u$ represents the mean value of the rectangular component of the E-field in an unloaded RC, P_{in} is the net input power to the RC. The normalized mean E-field (P_{in}=1 W) is shown in Fig. 3, which provides a useful reference to look up if a required E-field is expected. Once the mean value of the E-field is estimated, the peak value can be estimated by multiplying the mean value with a factor which depends on the independent sample number [3], [46]. When the loss is dominated by Q_{Tx} in (2) at low frequencies, the upper bound of the mean E-field can be obtained by substituting (4) into (8) which is $\sqrt{40\pi^3 P_{in}/\lambda^2}$ and is also plotted in Fig. 3. Note that there are some points exceed this limit, which should be due to the insufficient averaging or the RC works in the undermoded region and the field is no longer statistically uniform.

The effective conductivities of the RC walls are calculated and plotted in Fig. 4. The RC #8 is small and made of aluminum which shows the highest σ_{eff} and is relatively flat at high frequencies. This could be due to the fewer junctions between panels. Interestingly, the effective conductivity (σ_{eff}) of the walls shows frequency dependency and σ_{eff} shows higher values when the frequency increases. This could be due to the contact loss between panels of the wall. The #19, #22 and #35 RCs are from the same supplier, and the Q factors are measured

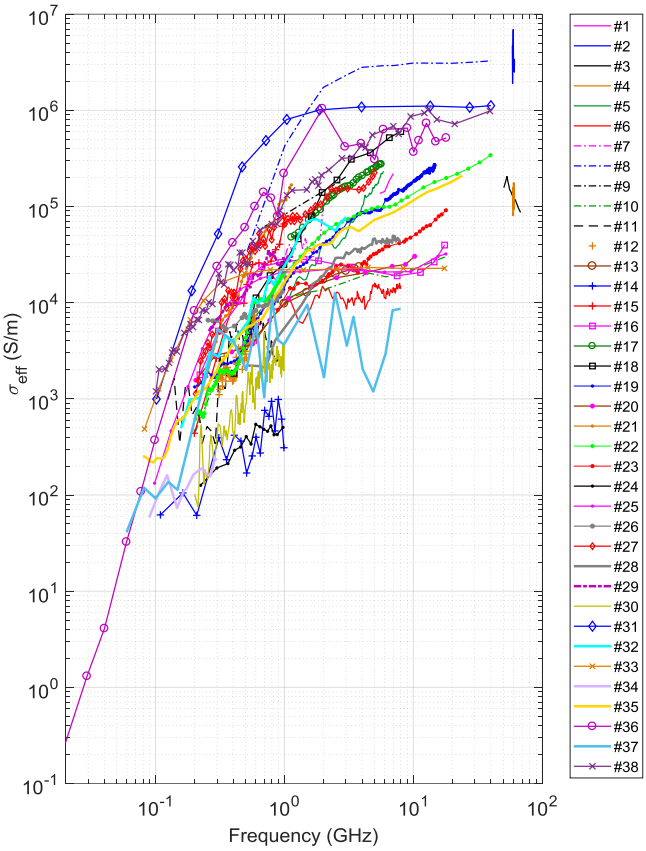

Fig. 4. Effective conductivity of the walls of different RCs.

using the time domain technique [50], [64]. It can be found that the calculated σ_{eff} (extracted and shown in Fig. 5) for these three RCs have good consistencies with each other as they are from the same supplier and the wall materials are the same. In the meanwhile, σ_{eff} of these three RCs locates nearly in the middle of all the curves in Fig. 4. To have an empirical equation conservatively, the least-squares fitting is performed for the minimum values of σ_{eff} from #19, #22 and #35 RCs in the frequency range of 100 MHz – 40 GHz in Fig. 5. Since the information of the measurement setup for the RCs in the literatures is incomplete, the low σ_{eff} in Fig. 4 could be due to the following reasons:

1) The Q factor is measured in the frequency domain and the total efficiency of antennas is not corrected accurately;
2) The σ_{eff} of these RCs is indeed low;
3) The RC is actually loaded (with wood, foam or other lossy objects).

IV. Discussion

The loss in an RC using the wall loss with effective conductivity has been emulated. However, the model used in this paper is equivalent to the conductive air model. Suppose the permittivity of the conductive air inside an RC is $\varepsilon = \varepsilon' - j\varepsilon''$, we have

$$\tan\delta = \frac{\varepsilon''}{\varepsilon'} = \frac{\varepsilon_r''}{\varepsilon_r'} = \frac{\sigma_{\text{diel}}}{\omega\varepsilon_r'\varepsilon_0} \tag{9}$$

The Q factor contributed by the lossy air is [81]

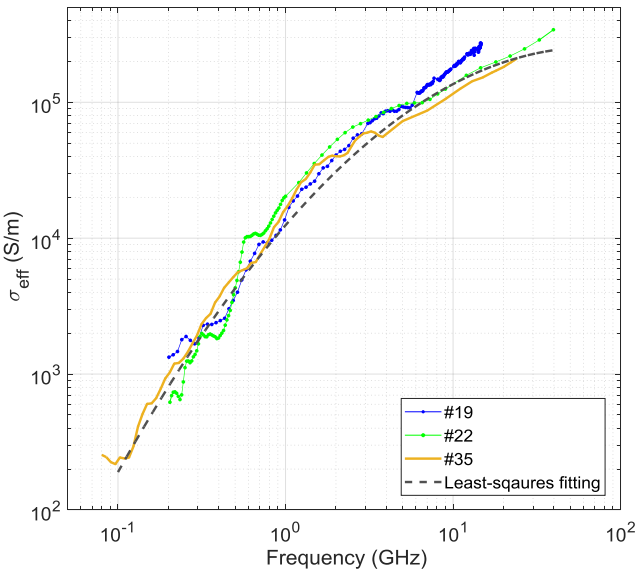

Fig. 5. The effective conductivity of the walls of the RCs from the same supplier with different dimensions. The least-squares fitting equation is $y = -0.04x^2 + 1.43x + 40.95$, where $x = 10\log_{10}(f)$, f in GHz and $y = 10\log_{10}(\sigma_{\text{eff}})$, σ_{eff} in S/m.

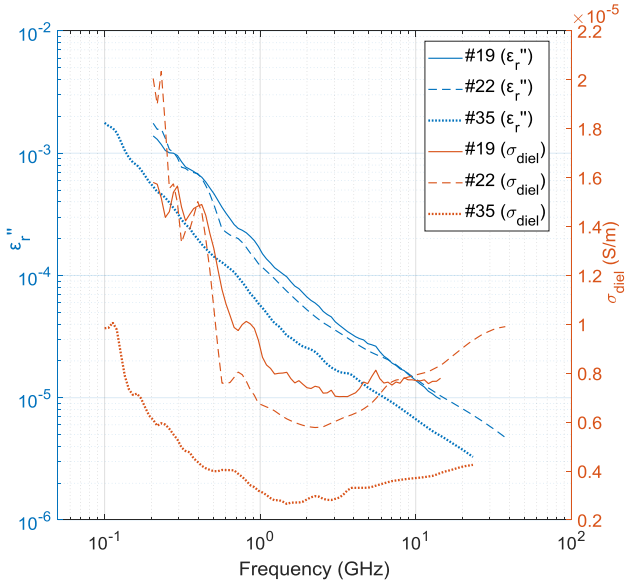

Fig. 6. The equivalent conductive air model: the imaginary parts of the relative permittivity of the conductive air are calculated, the conductivities are also given.

$$Q_{\text{diel}} = \frac{1}{\tan\delta} = \frac{\varepsilon_r'}{\varepsilon_r''} \tag{10}$$

where $\varepsilon' = \varepsilon_r'\varepsilon_0$, $\varepsilon'' = \varepsilon_r''\varepsilon_0 = \sigma_{\text{diel}}/\omega$, ε_r' and ε_r'' are the relative real part and imaginary part of the permittivity, respectively, $\varepsilon_0 \approx 8.85 \times 10^{-12}$ F/m is the permittivity of free space, σ_{diel} is the conductivity of the lossy air inside the RC. When $\varepsilon_r' = 1$, the total Q factor of the RC can be written as $Q^{-1} = Q_{\text{diel}}^{-1} + Q_{\text{Tx}}^{-1} + Q_{\text{Rx}}^{-1}$, when the contribution from the loss of the antennas is small, we have

$$Q^{-1} \approx Q_{\text{diel}}^{-1}, \text{or } \varepsilon_r'' \approx Q^{-1} \tag{11}$$

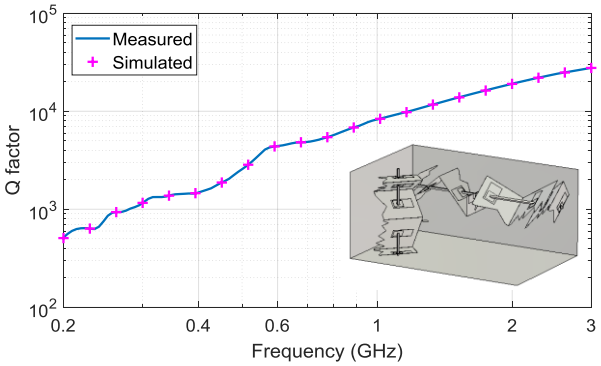

Fig. 7. A comparison of measured and simulated Q factor of RC #22.

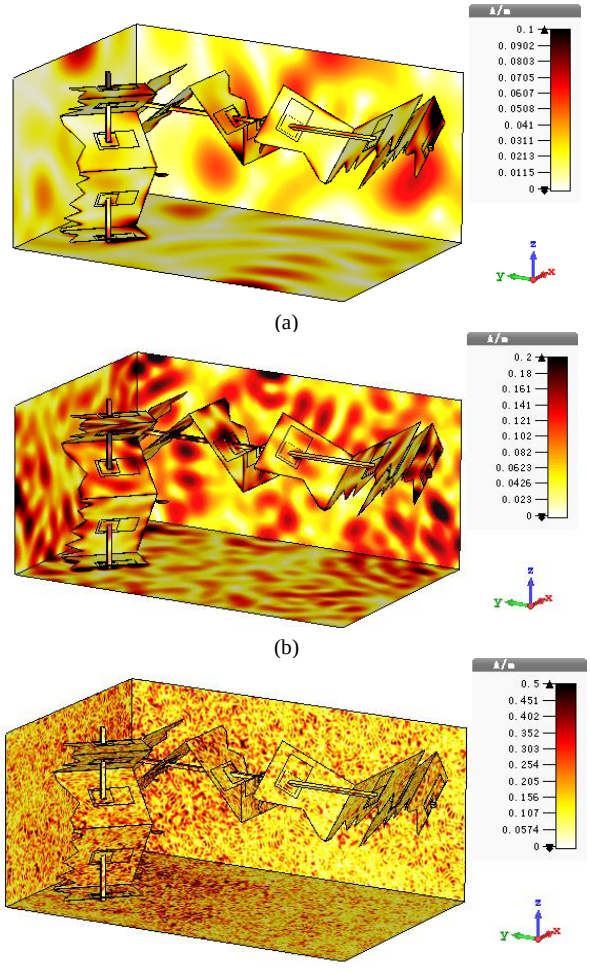
(a)

(b)

(c)

Fig. 8. Simulated surface current density (or H-field) at different frequencies: (a) 0.2 GHz, (b) 0.4 GHz and (c) 3 GHz.

The equivalency between the loss from the lossy air and the conductive wall parameters can be found using $Q_{\text{diel}} = Q_w$ in (3) which are

$$\varepsilon_r'' = \frac{2\mu_r S}{3V}\left[1 + \frac{3\pi}{8k}\left(\frac{1}{a} + \frac{1}{b} + \frac{1}{d}\right)\right]\sqrt{2/(\omega\mu\sigma_{\text{eff}})}$$

$$\approx \frac{2\mu_r S\sqrt{2/(\omega\mu\sigma_{\text{eff}})}}{3V} \qquad (12)$$

and $\sigma_{\text{diel}} = \omega\varepsilon_r''\varepsilon_0$. The calculated ε_r'' and σ_{diel} from σ_{eff} in Fig. 5 are illustrated in Fig. 6. The values of σ_{diel} in Fig. 6 are also in the same order with the typical value of 10^{-5} S/m used in [12]-[15]. To validate the equivalency of the conductive air model, we use the calculated ε_r'' (or σ_{diel}) of RC #22 and simulate the Q factors. The simulated results are presented in Fig. 7. As expected, accurate Q factors are reconstructed in the simulation model. The FEM method is used to simulate the model with a tetrahedron number of 19,038,722, and the peak memory consumption is about 210.7 GB. As the memory consumption is huge, we did not simulate the model for frequencies higher than 3 GHz. The surface current density (or H-field) for different frequencies is illustrated in Fig. 8. Unlike in measurements, the Q factors in simulations can be postprocessed from the fields inside the RC using (1) directly.

Although conductive air model and the lossy wall model are theoretically equivalent in emulating loss in RCs, the conductive wall model can give stable values (σ_{eff}) for different RCs as shown in Fig. 5. The parameters ε_r'' (or σ_{diel}) in the lossy air model depends on the volume of the RC and a larger volume gives smaller values. This can also be found in (12), unlike the conductive wall model, the parameters for the lossy air model vary for different RC dimensions. A more general and complex model has been proposed in [82] to include the loss from permeability (without the assumption of $\mu_r = 1$), and a multi-layer wall model is used. The multi-layer model should be closer to real physical world but more complex.

V. Conclusions

Estimating the unloaded Q factor of an RC before measurements is a long-standing problem in practice. This problem is difficult to solve from pure simulations. Thanks to the existing RCs worldwide, this problem can now be answered by adapting an engineering approach.

In 1980, the Q factor of 7 RCs had been reviewed [83]. This paper has reviewed the unloaded Q factors of 38 RCs from published literatures, and calculated the relevant effective wall conductivities (σ_{eff}). The σ_{eff} of three RCs from the same supplier with different dimensions have been measured. The results show good consistencies and an empirical equation has been given. Since the aim is to provide estimated σ_{eff} values, the surface area of the stirrers inside the RCs are not considered. As for large RCs, the surface area of stirrers is small compared with the overall internal surface area. The #19 and #22 RCs have horizontal and vertical stirrers while the #35 RC has an oscillating wall stirrer, but they give similar σ_{eff}. The equivalency between the conductive wall model and the lossy air model is also discussed. The parameters for the lossy air model show dependency on the dimensions of an RC and may not be easily generalized to arbitrary dimensions.

Although the focus is given on the galvanized steel RCs, one should note that σ_{eff} for all the RCs are not the same. This is not surprising, as different RC supplier may have different surface material and different ways to connect panels. From this paper, a reference σ_{eff} has been given, and it is believed that σ_{eff}

should be stable for the same supplier (with the same material and consistent panel connections). This information is envisaged useful for an RC supplier. For customized RC dimensions, the proposed empirical equations could provide references to estimate the mean E-field conservatively.

REFERENCES

[1] H. A. Mendes, *A new approach to electromagnetic field-strength measurements in shielded enclosures*, Wescon Technical Papers, Wescon Electronic Show and Convention, Los Angeles, 1968.

[2] M. Migliaccio, G. Gradoni and L. R. Arnaut, "Electromagnetic reverberation: the legacy of Paolo Corona," *IEEE Transactions on Electromagnetic Compatibility*, vol. 58, no. 3, pp. 643-652, Jun. 2016.

[3] IEC 61000-4-21, *Electromagnetic compatibility (EMC) – Part 4-21: Testing and measurement techniques – Reverberation chamber test methods*, IEC Standard, Ed 2.0, 2011-01.

[4] CTIA, *Test Plan for Wireless Large-Form-Factor Device Over-the-Air Performance*, ver. 1.2.1, Feb. 2019.

[5] D. A. Hill, *Electromagnetic Fields in Cavities: Deterministic and Statistical Theories*, Wiley-IEEE Press, USA, 2009.

[6] S. F. Romero, G. Gutierrez and I. Gonzalez, "Prediction of the maximum electric field level inside a metallic cavity using a quality factor estimation," *Journal of Electromagnetic Waves and Applications,* vol. 28, no. 12, pp. 1468-1477, 2014.

[7] K. Harima and Y. Yamanaka, "FDTD analysis on the effect of stirrers in a reverberation chamber," *International Symposium on Electromagnetic Compatibility*, Tokyo, Japan, 1999, pp. 260-263.

[8] J. Kim and R. Mittra, "Performance evaluation of a mode-stirred reverberation chamber using the finite difference time domain (FDTD) simulation," *Asia-Pacific Symposium on Electromagnetic Compatibility*, Singapore, 2012, pp. 173-176.

[9] V. M. Primiani and F. Moglie, "Reverberation chamber performance varying the position of the stirrer rotation axis," *IEEE Transactions on Electromagnetic Compatibility*, vol. 56, no. 2, pp. 486-489, Apr. 2014.

[10] L. Bastianelli, V. M. Primiani and F. Moglie, "Stirrer efficiency as a function of its axis orientation," *IEEE Transactions on Electromagnetic Compatibility*, vol. 57, no. 6, pp. 1732-1735, Dec. 2015.

[11] G. Gradoni, V. M. Primiani and F. Moglie, "Dependence of reverberation chamber performance on distributed losses: A numerical study," *IEEE International Symposium on Electromagnetic Compatibility (EMC)*, Raleigh, USA, 2014, pp. 775-780.

[12] F. Moglie, L. Bastianelli and V. M. Primiani, "Reliable finite-difference time-domain simulations of reverberation chambers by using equivalent volumetric losses," *IEEE Transactions on Electromagnetic Compatibility*, vol. 58, no. 3, pp. 653-660, Jun. 2016.

[13] F. Moglie and V. M. Primiani, "Reverberation chambers: full 3D FDTD simulations and measurements of independent positions of the stirrers," *IEEE International Symposium on Electromagnetic Compatibility*, Long Beach, USA, 2011, pp. 226-230.

[14] Y. Cui, G. Wei, S. Wang and L. Du, "Fast calculation of reverberation chamber Q-factor," *Electronics Letters*, vol. 48, no. 18, pp. 1116-1117, 30 Aug. 2012.

[15] S. Wang, Z. Wu, G. Wei, Y. Cui and L. Fan, "A new method of estimating reverberation chamber Q-factor with experimental validation," P*rogress In Electromagnetic Research Letter*, vol. 36, pp. 103-112, 2013.

[16] D. I. Wu and D. C. Chang, "The effect of an electrically large stirrer in a mode-stirred chamber," *IEEE Transactions on Electromagnetic Compatibility*, vol. 31, no. 2, pp. 164-169, May 1989.

[17] J. Clegg, A. C. Marvin, J. F. Dawson and S. J. Porter, "Optimization of stirrer designs in a reverberation chamber," *IEEE Transactions on Electromagnetic Compatibility*, vol. 47, no. 4, pp. 824-832, Nov. 2005.

[18] A. Coates, H. G. Sasse, D. E. Coleby, A. P. Duffy and A. Orlandi, "Validation of a three-dimensional transmission line matrix (TLM) model implementation of a mode-stirred reverberation chamber," *IEEE Transactions on Electromagnetic Compatibility*, vol. 49, no. 4, pp. 734-744, Nov. 2007.

[19] D. Weinzierl, A. Raizer, A. Kost and G. S. Ferreira, "Simulation of a mode stirred chamber excited by wires using the TLM method," *COMPEL – The International Journal for Computation and Mathematics in Electrical and Electronic Engineering*, vol. 22, no. 3, pp. 770–778, 2003.

[20] D. Weinzierl, C. A. F. Sartori, M. B. Perotoni, J. R. Cardoso, A. Kost and E. F. Heleno, "Numerical evaluation of noncanonical reverberation chamber configurations," *IEEE Transactions on Magnetics*, vol. 44, no. 6, pp. 1458-1461, Jun. 2008.

[21] H. -J. Asander, G. Eriksson, L. Jansson and H. Akermark, "Field uniformity analysis of a mode stirred reverberation chamber using high resolution computational modeling," *IEEE International Symposium on Electromagnetic Compatibility*, Minneapolis, USA, 2002, pp. 285-290.

[22] M. E. Gruber, S. B. Adrian and T. F. Eibert, "A finite element boundary integral formulation using cavity Green's function and spectral domain factorization for simulation of reverberation chambers," *International Conference on Electromagnetics in Advanced Applications (ICEAA)*, Torino, Italy, 2013, pp. 460-463.

[23] P. Leuchtmann, C. Bruns and R. Vahldieck, "Broadband method of moment simulation and measurement of a medium-sized reverberation chamber," *IEEE Symposium on Electromagnetic Compatibility*, Boston, USA, 2003, pp. 844-849 vol.2.

[24] C. Bruns and R. Vahldieck, "A closer look at reverberation chambers - 3-D simulation and experimental verification," *IEEE Transactions on Electromagnetic Compatibility*, vol. 47, no. 3, pp. 612-626, Aug. 2005.

[25] U. Carlberg, P. -S. Kildal and J. Carlsson, "Study of antennas in reverberation chamber using method of moments with cavity Green's function calculated by Ewald summation," *IEEE Transactions on Electromagnetic Compatibility*, vol. 47, no. 4, pp. 805-814, Nov. 2005.

[26] U. Carlberg, P. –S, Kildal and J. Carlsson, "Numerical study of position stirring and frequency stirring in a loaded reverberation chamber," *IEEE Transactions on Electromagnetic Compatibility*, vol. 51, no. 1, pp. 12-17, Feb. 2009.

[27] U. Carlberg, P. -S. Kildal and A. A. Kishk, "Fast numerical model of reverberation chambers with metal stirrers using moment method and cavity Green's function calculated by Ewald summation," *IEEE Antennas and Propagation Society International Symposium*, Albuquerque, USA, 2006, pp. 2827-2830.

[28] M. E. Gruber and T. F. Eibert, "A cavity Green's function boundary element method for the modeling of reverberation chambers: validation against measurements," *IEEE International Symposium on Electromagnetic Compatibility (EMC)*, Dresden, Germany, 2015, pp. 563-566.

[29] J. C. West, V. Rajamani and C. F. Bunting, "Practical considerations for the evaluation of the 3-D Green's function in a rectangular cavity moment method at high frequency," *IEEE International Symposium on Electromagnetic Compatibility*, Denver, USA, 2013, pp. 813-818.

[30] H. Zhao and Z. Shen, "Fast wideband analysis of reverberation chambers using hybrid discrete singular convolution-method of moments and adaptive frequency sampling," *IEEE Transactions on Magnetics*, vol. 51, no. 3, pp. 1-4, Mar. 2015.

[31] H. Zhao, "MLFMM-accelerated integral-equation modeling of reverberation chambers," *IEEE Antennas and Propagation Magazine*, vol. 55, no. 5, pp. 299-308, Oct. 2013.

[32] H. Zhao, E. Li and Z. Shen, "Modeling of reverberation chamber using FMM-accelerated hybrid integral equation," *IEEE Asia-Pacific Conference on Antennas and Propagation*, Singapore, 2012, pp. 213-214.

[33] C. F. Bunting, "Shielding effectiveness in a two-dimensional reverberation chamber using finite-element techniques," *IEEE Transactions on Electromagnetic Compatibility*, vol. 45, no. 3, pp. 548-552, Aug. 2003.

[34] C. F. Bunting, "Statistical characterization and the simulation of a reverberation chamber using finite-element techniques," *IEEE Transactions on Electromagnetic Compatibility*, vol. 44, no. 1, pp. 214-221, Feb. 2002.

[35] C. Suriano, G. A. Thiele and J. R. Suriano, "Predicting low frequency behavior of arbitrary reverberation chamber configurations," *International Symposium on Electromagnetic Compatibility*, Montreal, Canada, 2001, vol. 2, pp. 757-761.

[36] D. Zhang and E. Li, "Characterization of a reverberation chamber by 3D finite element method," *3rd International Symposium on Electromagnetic Compatibility*, Beijing, China, 2002, pp. 394-396.

[37] Y. Huang, J. Zhang and P. Liu, "A novel method to examine the effectiveness of a stirrer," *International Symposium on Electromagnetic Compatibility*, Chicago, USA, 2005, pp. 556-561.

[38] G. Orjubin, E. Richalot, S. Mengue and O. Picon, "Statistical model of an undermoded reverberation chamber," *IEEE Transactions on Electromagnetic Compatibility*, vol. 48, no. 1, pp. 248-251, Feb. 2006.

[39] G. Orjubin, E. Richalot, O. Picon and O. Legrand, "Chaoticity of a reverberation chamber assessed from the analysis of modal distributions

obtained by FEM," *IEEE Transactions on Electromagnetic Compatibility*, vol. 49, no. 4, pp. 762-771, Nov. 2007.
[40] G. Orjubin, E. Richalot, S. Mengue, M. Wong and O. Picon, "On the FEM modal approach for a reverberation chamber analysis," *IEEE Transactions on Electromagnetic Compatibility*, vol. 49, no. 1, pp. 76-85, Feb. 2007.
[41] C. L. Zekios, P. C. Allilomes and G. A. Kyriacou, "Eigenfunction expansion for the analysis of closed cavities," *Loughborough Antennas & Propagation Conference*, Loughborough, UK, 2010, pp. 537-540.
[42] C. L. Zekios, P. C. Allilomes, C. S. Lavranos and G. A. Kyriacou, "A three dimensional finite element eigenanalysis of reverberation chambers," *International Symposium on Electromagnetic Compatibility - EMC Europe*, Athens, 2009, pp. 1-4.
[43] C. L. Zekios, P. C. Allilomes, M. T. Chryssomallis, and G. A. Kyriacou, "Finite element based eigenanalysis for the study of electrically large lossy cavities and reverberation chambers," *Progress in Electromagnetics Research B*, vol. 61, pp. 269–296, 2014.
[44] C. Bruns, *Three-Dimensional Simulation and Experimental Verification of a Reverberation Chamber*, Doctor of Sciences Dissertation, Swiss Federal Institute of Technology Zuric, 2005.
[45] U. Carlberg P.-S. Kildal A. Wolfang O. Sotoudeh C. Orlenius "Calculated and measured absorption cross sections of lossy objects in reverberation chamber," *IEEE Transactions on Electromagnetic Compatibility*, vol. 46 no. 2 pp. 146-154 May 2004.
[46] Q. Xu, X. Shen, K. Chen, Y. Zhao and Y. Huang, "Absorption cross section measurement of a vehicle in reverberation chamber for quick estimation of field strength," *IEEE Electromagnetic Compatibility Magazine*, vol. 8, no. 4, pp. 44-49, 2019.
[47] J. Ladbury and D. A. Hill, "Enhanced backscatter in reverberation chamber: Inside every complex problem is a simple solution struggling to get out," *Proc. IEEE Int. Symp. Electromagn. Compat.*, Jul. 9–13, 2007, pp. 1–5.
[48] I. Junqua, P. Degauque, M. Liénard and F. Issac, "On the power dissipated by an antenna in transmit mode or in receive mode in a reverberation chamber," *IEEE Transactions on Electromagnetic Compatibility*, vol. 54, no. 1, pp. 174-180, Feb. 2012.
[49] C. R. Dunlap, *Reverberation Chamber Characterization using Enhanced Backscatter Coefficient Measurements*, Ph.D. dissertation, Dept. of Electrical, Computer and Engineering, University of Colorado, Boulder, USA, 2013.
[50] J. C. West, J. N. Dixon, N. Nourshamsi, D. K. Das and C. F. Bunting, "Best practices in measuring the quality factor of a reverberation chamber," *IEEE Transactions on Electromagnetic Compatibility*, vol. 60, no. 3, pp. 564-571, Jun. 2018.
[51] B. -H. Liu and M. T. Ma, *Eigenmodes and the Composite Quality Factor of a Reverberating Chamber*, NBS Technical Note 1066, 1983.
[52] N. Nourshamsi, J. C. West and C. F. Bunting, "Required bandwidth for time-domain measurement of the quality factor of reverberation chambers," *IEEE International Symposium on Electromagnetic Compatibility &* Signal/Power Integrity (EMCSI), Washington, DC, 2017, pp. 481-485.
[53] A. K. Fall, P. Besnier, C. Lemoine, M. Zhadobov and R. Sauleau, "Design and experimental validation of a mode-stirred reverberation chamber at millimeter waves," *IEEE Transactions on Electromagnetic Compatibility*, vol. 57, no. 1, pp. 12-21, Feb. 2015.
[54] F. Santoni, R. Pastore, G. Gradoni, F. Piergentili, D. Micheli, R. Diana and A. Delfini, "Experimental characterization of building material absorption at mmWave frequencies: by using reverberation chamber in the frequency range 50–68 GHz," *IEEE Metrology for Aerospace (MetroAeroSpace)*, Florence, 2016, pp. 166-171.
[55] R. Aminzadeh, J. Sol, P. Besnier, M. Zhadobov, L. Martens and W. Joseph, "Estimation of average absorption cross section of a skin phantom in a mm-Wave reverberation chamber," *13th European Conference on Antennas and Propagation (EuCAP)*, Krakow, Poland, 2019, pp. 1-3.
[56] Q. Xu and Y. Huang, *Anechoic and Reverberation Chambers: Theory, Design and Measurements*, Wiley-IEEE, 2019.
[57] D. Senic, A. Šarolić, Z. M. Jóskiewicz and C. L. Holloway, "Absorption cross-section measurements of a human model in a reverberation chamber," *IEEE Transactions on Electromagnetic Compatibility*, vol. 58, no. 3, pp. 721-728, Jun. 2016.
[58] K. W. Jin, F. W. Jian and N. Y. Seng, "RC for pulse HIRF testing," *Asia-Pacific International Symposium on Electromagnetic Compatibility (APEMC)*, Shenzhen, China, 2016, pp. 335-337.
[59] F. Monsef and A. Cozza, "Average number of significant modes excited in a mode-stirred reverberation chamber," *IEEE Transactions on Electromagnetic Compatibility*, vol. 56, no. 2, pp. 259-265, Apr. 2014.
[60] J. Ladbury, G. Koepke, and D. Camell, "Evaluation of the NASA Langley research center mode-stirred chamber facility," *NIST Technical Note 1508*, 1999.
[61] L. L. Bars, J. Rosnarho, P. Besnier, J. Sol, F. Sarrazin and E. Richalot, "Geometry and loading effects on performances of mode-stirred reverberation chambers: an experimental study," *International Symposium on Electromagnetic Compatibility - EMC EUROPE*, Barcelona, Spain, 2019, pp. 163-168.
[62] R. V-. Ardatjew, U. Lundgren, S. F. Romero and F. Leferink, "On-site radiated emissions measurements in semireverberant environments," *IEEE Transactions on Electromagnetic Compatibility*, vol. 59, no. 3, pp. 770-778, Jun. 2017.
[63] A. Kadri, D. C. Pande and A. Mishra, "Analysis of a mechanically stirred reverberation chamber," *15th International Conference on ElectroMagnetic Interference & Compatibility (INCEMIC)*, Bengaluru (Bangalore), India, 2018, pp. 1-4.
[64] C. L. Holloway, H. A. Shah, R. J. Pirkl, W. F. Young, D. A. Hill and J. Ladbury, "Reverberation chamber techniques for determining the radiation and total efficiency of antennas," *IEEE Transactions on Antennas and Propagation*, vol. 60, no. 4, pp. 1758-1770, Apr. 2012.
[65] H. Vallon, A. Chauchat, F. Monsef and A. Cozza, "Effect of loading a mode-stirred chamber with antennas on Q-factor and comparison to theory," *XXXIth URSI General Assembly and Scientific Symposium (URSI GASS)*, Beijing, China, 2014, pp. 1-4.
[66] V. Creta, L. Bastianelli, F. Moglie, V. M. Primiani and L. R. Arnaut, "Stirring performance of helically distributed paddles," *IEEE International Symposium on Electromagnetic Compatibility & Signal/Power Integrity (EMCSI)*, Washington, USA, 2017, pp. 670-674.
[67] L. A. Bronckers, A. Roc'h and A. B. Smolders, "Reverberation chamber enhanced backscattering: high-frequency effects," *International Symposium on Electromagnetic Compatibility - EMC EUROPE*, Barcelona, Spain, 2019, pp. 1-6.
[68] J. Ji, X. Zhou and P. Hu, "Frequency-dependent oscillating wall stirrer for measurement of quality factor in a reverberation chamber," *IEEE International Conference on Computation, Communication and Engineering (ICCCE)*, Fujian, China, 2019, pp. 142-145.
[69] C. Li, T. Loh, Z. H. Tian, Q. Xu and Y. Huang, "A comparison of antenna efficiency measurements performed in two reverberation chambers using non-reference antenna methods," *Loughborough Antennas & Propagation Conference (LAPC)*, Loughborough, UK, 2015, pp. 1-5.
[70] Z. Tian, Y. Huang, Q. Xu, T. Loh and C. Li, "Measurement of absorption cross section of a lossy object in reverberation chamber without the need for calibration," *Loughborough Antennas & Propagation Conference (LAPC)*, Loughborough, UK, 2016, pp. 1-5.
[71] P. Besnier, C. Lemoine and J. Sol, "Various estimations of composite Q-factor with antennas in a reverberation chamber," *IEEE International Symposium on Electromagnetic Compatibility (EMC)*, Dresden, Germany, 2015, pp. 1223-1227.
[72] T. H. Loh and K. Liu, "Routing and link performance assessment of a wireless sensor network in a reverberation chamber with different absorber loading condition," *XXXIInd General Assembly and Scientific Symposium of the International Union of Radio Science (URSI GASS)*, Montreal, Canada, 2017, pp. 1-4.
[73] L. R. Arnaut, "Statistics of the quality factor of a rectangular reverberation chamber," *IEEE Transactions on Electromagnetic Compatibility*, vol. 45, no. 1, pp. 61-76, Feb. 2003.
[74] J. Kasper, M. Magdowski and R. Vick, "Comparison of the field-to-wire coupling to bent and curved transmission lines in reverberation chambers," *International Symposium on Electromagnetic Compatibility (EMC EUROPE)*, Amsterdam, Netherlands , 2018, pp. 713-718.
[75] M. Pocai, I. Dotto, D. Festa and G. D'Abreu, "Improving the performances of a reverberation chamber: a real case," *20th International Zurich Symposium on Electromagnetic Compatibility*, Zurich, Switzerland, 2009, pp. 53-56.
[76] Y. Zhao, G. Wei, Y. Cui, L. Fan, X. Pan and H. Wan, "Acceleration technique of modeling lossy reverberation chamber using FDTD method based on quality factor," *IEEE Antennas and Wireless Propagation Letters*, vol. 14, pp. 686-689, 2015.
[77] P. A. Johnson and K. R. Goldsmith, "An experimental study of the placement of an aircraft inside a large welded zinc-plated steel electromagnetic reverberation chamber," *17th DASC. AIAA/IEEE/SAE. Digital Avionics Systems Conference*, Bellevue, USA, 1998, vol.1, pp. D42/1-D42/9.
[78] K. R. Goldsmith and P. A. Johnson, "Design, construction, computational EM modelling, and characterisation of an aircraft sized reverberation

chamber and stirrer," *17th DASC. AIAA/IEEE/SAE. Digital Avionics Systems Conference*, Bellevue, USA, 1998, vol.1, pp. D55/1-D55/8.
[79] M. O. Hatfield, G. J. Freyer and M. B. Slocum, "Reverberation characteristics of a large welded steel shielded enclosure," *International Symposium on Electromagnetic Compatibility*, Austin, USA, 1997, pp. 38-43.
[80] C. L. Lewis, R. J. Dolesh and M. J. Garrett, "Space power facility reverberation chamber calibration report," *NASA Technical Reports*, NASA/TM-2014-218363, 2014.
[81] M. Popovic, A. Moretti, C. M. Ankenbrandt, M. A. C. Cummings, R. P. Johnson and M. Neubauer, "RF cavities with dielectric for muon facilities," *Proceedings of PAC09*, Vancouver, Canada, 2009, pp. 846-848.
[82] A. Cozza and F. Monsef, "Power dissipation in reverberation chamber metallic surfaces based on ferrous materials," *IEEE Transactions on Electromagnetic Compatibility*, vol. 61, no. 6, pp. 1714-1725, Dec. 2019.
[83] P. Corona, G. Latmiral and E. Paolini, "Performance and analysis of a reverberating enclosure with variable geometry," *IEEE Transactions on Electromagnetic Compatibility*, vol. 22, no. 1, pp. 2-5, Feb. 1980.

Qian Xu received the B.Eng. and M.Eng. degrees from the Department of Electronics and Information, Northwestern Polytechnical University, Xi'an, China, in 2007 and 2010, and received the PhD degree in electrical engineering from the University of Liverpool, U.K, in 2016. He is currently an Associate Professor at the College of Electronic and Information Engineering, Nanjing University of Aeronautics and Astronautics, China.

He was as a RF engineer in Nanjing, China in 2011, an Application Engineer at CST Company, Shanghai, China in 2012. His work at University of Liverpool was sponsored by Rainford EMC Systems Ltd. (now part of Microwave Vision Group) and Centre for Global Eco-Innovation. He has designed many chambers for the industry and has authored the book *Anechoic and Reverberation Chambers: Theory, Design, and Measurements* (Wiley-IEEE, 2019). His research interests include statistical electromagnetics, reverberation chamber, computational electromagnetics, and anechoic chamber.

Lei Xing received the B.Eng. and M.Eng. degrees from the School of Electronics and Information, Northwestern Polytechnical University, Xi'an, China, in 2009 and 2012. She received PhD degree in electrical engineering and electronics at the University of Liverpool, U.K, in 2015. She is currently an Associate Professor at the College of Electronic and Information Engineering, Nanjing University of Aeronautics and Astronautics, China.

Yongjiu Zhao received the M.Eng. and Ph.D. degrees in electronic engineering from Xidian University, Xi'an, China, in 1990 and 1998, respectively. Since March 1990, he has been with the Department of Mechano-Electronic Engineering, Xidian University where he was a Professor in 2004. From December 1999 to August 2000, he was a Research Associate with the Department of Electronic Engineering, The Chinese University of Hong Kong. From 2007, he is a Professor in Electromagnetics and Deputy Head of the Department at the College of Electronic and Information Engineering, Nanjing University of Aeronautics and Astronautics.

Xinlei Chen (M'14) was born in Xuzhou, Jiangsu, China, in 1984. He received the B.S. degree in electronic information science and technology, the M.E. degree in electromagnetic field and microwave technology, and the Ph.D. degree in communication and information system from the Nanjing University of Aeronautics and Astronautics (NUAA), Nanjing, China, in 2007, 2010, and 2015, respectively.

Yi Huang (S'91– M'96 – SM'06 – F'20) received BSc in Physics (Wuhan University, China) in 1984, MSc (Eng) in Microwave Engineering (NRIET, Nanjing, China) in 1987, and DPhil in Communications from the University of Oxford, UK in 1994.

He has been conducting research in the areas of wireless communications, applied electromagnetics, radar and antennas since 1987. His experience includes 3 years spent with NRIET (China) as a *Radar Engineer* and various periods with the Universities of Birmingham, Oxford, and Essex at the UK as a member of research staff. He worked as a Research Fellow at British Telecom Labs in 1994, and then joined the Department of Electrical Engineering & Electronics, the University of Liverpool, UK as a Faculty in 1995, where he is now a full Professor in Wireless Engineering, the Head of High Frequency Engineering Group and Deputy Head of Department.

Xueqi Shen received the M.Eng. degree from the Department of Radio at Southeast University in Nanjing, China, in 1989. He founded Rongxiang Company in 2004 and the EMC testing laboratory Nanjing Rongce in Nanjing in 2012 which is a recognized EMC Lab by Ford and Yutong. Currently, Nanjing Rongce has the largest vehicle reverberation chamber in China. He is a committee member of Branches A, I, and D of the National Technical Committee on Radio Interference of Standardization Administration of China.

Mark Paul Leach received the BEng (Hons) in Communication and Electronic Engineering from the University of Northumbria, UK in 1999 and Ph.D from the same institution in 2005. Dr. Leach worked as a research associate from 2003 to 2008 in the field of Microwave

Holography. From 2008 – 2013, Dr. Leach was employed as a lecturer at Seoul National University of Science and Technology, conducting research into thin films for photovoltaic applications. In 2013 Dr. Leach joined the Department of Electrical and Electronic Engineering at Xi'an Jiaotong Liverpool University where he is now head of department.

Eng Gee Lim received the BEng (Hons) and PhD degrees in Electrical and Electronic Engineering from the UK. Prof. Lim worked for Andrew Ltd, a leading communications systems company in the United Kingdom from 2002 to 2007. Since August 2007, Prof. Lim has been at Xi'an Jiaotong Liverpool University, where he was formally the head of EEE department and University Dean of Research and Graduate studies. Now, he is School Dean of Advanced Technology, director of AI university research centre and also professor in department of Electrical and Electronic Engineering. He is a charter engineer and Fellow of both IET and Engineers Australia. In addition, he is also a senior member of IEEE and Senior Fellow of HEA.

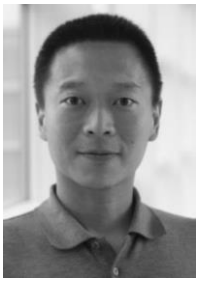

Tian-Hong Loh (S'03–M'05–SM'15) received the Ph.D. degree in engineering from the University of Warwick, UK in 2005. He has been with the UK National Physical Laboratory (NPL) since 2005 as a Higher Research Scientist (2005 – 2009) and Senior Research Scientist (2009 - 2017). He is currently a Principal Research Scientist at NPL. He leads work at NPL on a wide range of applied and computational electromagnetic metrology research areas to support the telecommunications industry. He has authored and co-authored over hundred and fifty refereed publications and holds five patents. He is currently visiting professor at Surrey University, UK, visiting industrial fellow at Cambridge University, UK, UK representative of URSI Commission A (Electromagnetic Metrology), and project coordinator of an EU H2020 co-funded project on 'Metrology for 5G Communications', member of IET and senior member of the IEEE. He is an associate editor of IET Communications, IET Microwave, Antennas and Propagation Journal and the URSI Radio Science Bulletin for Commission A, and was the TPC chair of 2017 IEEE International Workshop on Electromagnetics. He has been a keynote/invited speaker of many conferences and workshops. He also has acted on the session chair and technical programme committee for several international conferences, and as technical reviewer for several international journals on these subjects. His research interests include 5G communications, multiple-input-multiple-output communications, smart antennas, small antennas, metamaterials, body-centric communications, wireless sensor network, electromagnetic compatibility, and computational electromagnetics.